Author's Accepted Manuscript

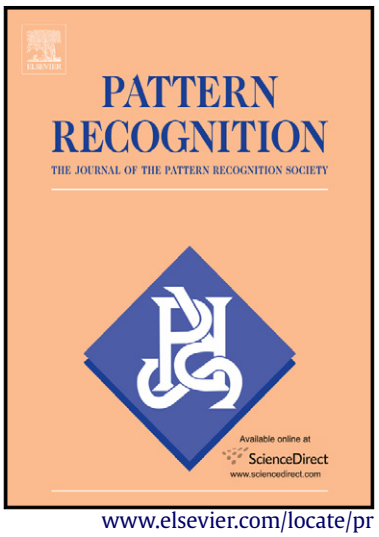

www.elsevier.com/locate/pr

Principles of time–frequency feature extraction for change detection in non-stationary signals: Applications to newborn EEG abnormality detection

Boualem Boashash, Ghasem Azemi, Nabeel Ali Khan

PII: S0031-3203(14)00330-6
DOI: http://dx.doi.org/10.1016/j.patcog.2014.08.016
Reference: PR5199

To appear in: *Pattern Recognition*

Received date: 30 January 2014
Revised date: 7 August 2014
Accepted date: 18 August 2014

Cite this article as: Boualem Boashash, Ghasem Azemi, Nabeel Ali Khan, Principles of time–frequency feature extraction for change detection in non-stationary signals: Applications to newborn EEG abnormality detection, *Pattern Recognition,* http://dx.doi.org/10.1016/j.patcog.2014.08.016

Principles of time–frequency feature extraction for change detection in non-stationary signals: applications to newborn EEG abnormality detection

Boualem Boashash[a,b], Ghasem Azemi[*,b], Nabeel Ali Khan[a]

[a] *Department of Electrical Engineering, Qatar University, Doha, Qatar.*
[b] *The University of Queensland, Centre for Clinical Research and Perinatal Research Centre, Royal Brisbane & Women's Hospital, Herston, QLD 4029, Australia.*

Abstract

This paper considers the general problem of detecting change in non-stationary signals using features observed in the time–frequency (t, f) domain, obtained using a class of quadratic time–frequency distributions (QTFDs). The focus of this study is to propose a methodology to define new (t, f) features by extending time-only and frequency-only features to the joint (t, f) domain for detecting changes in non-stationary signals. The (t, f) features are used as a representative subset characterizing the status of the observed non-stationary signal. Change in the signal is then reflected as a change in the (t, f) features. This (t, f) approach is applied to the problem of detecting abnormal brain activity in newborns (e.g. seizure) using measurements of the EEG for diagnosis and prognosis. In addition, a pre-processing stage for detecting artifacts in EEG signals for signal enhancement is studied and implemented separately. Overall results indicate that, in general, the (t, f) approach results in an improved performance in detecting artifacts and seizures in newborn EEG signals as compared to time-only or frequency-only features.

Key words: time–frequency feature extraction, abnormality detection, seizure, newborn EEG artifacts, ROC analysis

*Corresponding author
Email addresses: boualem@qu.edu.qa (Boualem Boashash), g.azemi@uq.edu.au (Ghasem Azemi), nabeelalikhan@qu.edu.qa (Nabeel Ali Khan)

1. Introduction

1.1. Change detection in non-stationary signals

Change detection in signals is the process of identifying differences in the state of an object or phenomenon by observing the signal generated by the process at different times. It has attracted widespread interest due to a large number of applications in diverse disciplines, including medical diagnosis [1, 2].

The goal of this study is to propose and test new features that can be used to detect changes in non-stationary signals that appear because of transition of an object from a normal state to an abnormal state or from one abnormal state to another abnormal state. For example, the appearance of seizure in EEG signals is a transition from a normal state to an abnormal state that can result in death or long term handicap. For applications involving non-stationary signals for which the spectral characteristics change with time, time–frequency (t, f) methods have proved a valuable tool based on their ability to highlight and describe such time–varying characteristics [1]. For such signals, time–frequency distributions (TFDs) allow greater insight into the nature of the information carried by the signal. In particular, TFD's ability to show how the energy of the signal is distributed over the 2D (t, f) domain helps identify important features such as the number of signal components, rate of change, and regions of energy concentration. In general, such information cannot be obtained directly from signals representations in time or frequency domains and therefore it is desired to test the hypothesis that (t, f) methods should allow for more accurate change detection in non-stationary signals. For these reasons, this paper aims to present (t, f) features that are extracted from the TFD of a signal and exploit the additional information provided by signal variations in terms of non-stationarities observed in the (t, f) domain. Such (t, f) features can therefore be considered suitable for monitoring and change detection in non-stationary

signals.

1.2. Paper contributions and organization

The main technical novelties of this study are three-fold: first, it introduces new (t, f)-based features suitable for change detection in non-stationary signals. Second, it presents a methodology for extending time–domain (t-domain) and frequency–domain (f-domain) features to the joint (t, f) domain. Third, it uses the introduced features to detect changes in EEG signals such as those caused by the presence of artifacts and brain abnormal activities.

Without loss of generality, this paper considers an illustrative application on a specific biomedical signal, namely, the newborn electroencephalography (EEG), and presents methodologies for detecting changes in the internal structure of signals as well as changes caused by external corrupting artifacts. As the signal characteristics vary in the transition from normal EEG to abnormal EEG, change detection techniques can be applied to newborn EEG signals for automatic diagnosis of abnormal brain activities and for signal enhancement. Traditional methods for detecting changes in EEG signals mostly concentrate on visual inspection which is a laborious and time-consuming task especially in the case of long recordings [1]. It also requires skilled interpreters; i.e. a neurophysiologist, who could be prone to subjective judgment and error that can result in serious consequences such as death or long term handicap. This paper tests the 2 point hypothesis that a) TFDs are well–adapted for detecting variations such as EEG abnormalities [1, 3] using a combined (t, f) pattern recognition and machine learning approach, and b) that an improved performance can be obtained when we replace t-domain or f-domain features by their corresponding extended (t, f) features.

The design of an automatic abnormality pattern recognition system requires defining representations that are suitable to show these abnormality patterns in a clear way using a range of

features, as well as allow feature extraction and selection. For the case of detection of newborn EEG abnormalities, the results in this paper confirm that TFDs and (t, f) based features can result in a reliable and accurate recognition system which is an improvement upon time–only or frequency–only features. A receiver operating characteristics (ROC) analysis is selected as a performance metric to evaluate the performance of each (t, f) feature when used to detect changes in newborn EEG signals. A comparison is also made between the performance of the (t, f) features extracted from different quadratic TFDs (QTFDs) including the extended modified B-distribution (EMBD) [1, 4]. The results of applying those features to data sets of newborn EEG signals marked for seizures reveal that the selected (t, f) features consistently result in a high degree of discrimination between different states in the signals. Further, a baseline comparison between time–only or frequency–only features and their translated extended (t, f) features show that the latter can improve the detection performance, thus justifying the (t, f) approach selected in this paper and verifying the research hypothesis.

The rest of the paper is organized as follows. Section 2 reviews relevant background about EEG signals. In Section 3, methodologies for automatic detection of artifacts and seizures in newborn EEG signals are described, including the key formulation of the (t, f) features. The results of applying such methodology to real data are provided in Section 4 and Section 5 concludes.

2. Newborn EEG signals

2.1. Newborn EEG seizures

EEG is the recording of brain electrical activities measured by electrodes placed on the scalp (see Figure 1). As EEG signals can be collected non-invasively and most brain related abnormalities show clear abnormal variations on EEG recordings, they are widely used for assessment

Figure 1: Recording newborn EEG signals.

of brain diseases and disorders [1]. Previous studies have shown that background EEG activities often provide objective evidence of the degree and severity of the underlying cause and that abnormal activities are correlated with adverse physical and/or neurological outcomes. Specifically in newborns, the presence of seizures carry with them a high probability of poor neurodevelopmental outcome or even death [5]. Newborn EEG seizures exhibit variations in voltage, duration, frequency content, and waveform shape (see illustrative example in Figure 2).

Techniques for automatic seizure detection using EEG signals include the use of time–domain statistics [6], spectral features [7], combination of time–only (t-only) with frequency–only (f-only) features [8], autoregressive (AR) modeling [9, 10], and non–linear analysis [11]. The above are limited in their performance as they do not take into account the property of non-stationarity, and instead they use the assumption of stationarity. Previous studies have shown that (t, f) based techniques which account for non-stationarities have superior performance for detecting seizures in newborn EEG signals [12, 13, 14]. These findings motivated the need to define and assess the performance of the (t, f) features presented in Section 3.3.3 for automatic seizure detection in

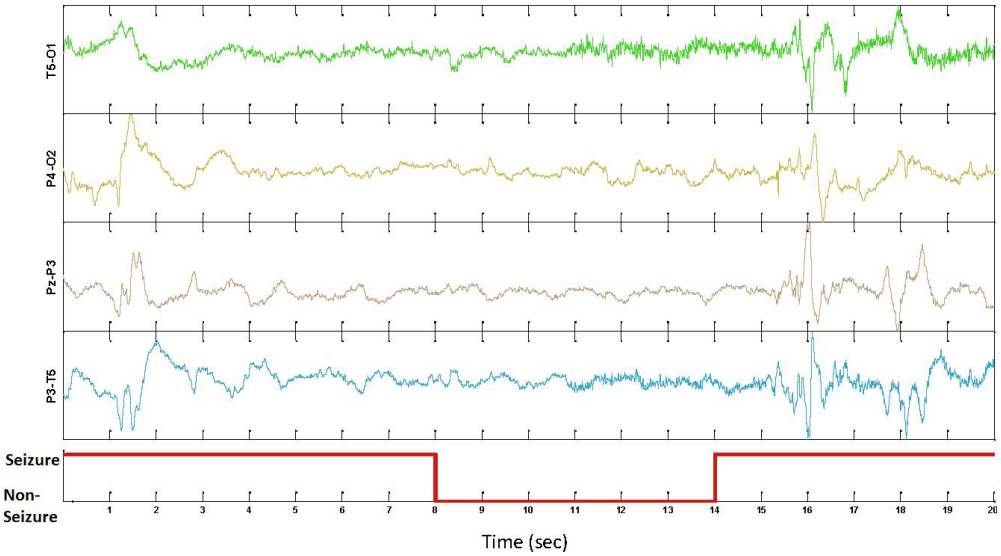

Figure 2: EEG of a newborn showing seizure patterns. *The plot at the bottom shows the binary mask prepared based on the clinical observation of a pediatric neurologist. Note that only 4 EEG channels (out of 20 recorded EEG channels) displaying clear seizure patterns are shown in the figure.*

newborn EEG.

2.2. Newborn EEG Artifact Detection

A major problem with the implementation of a fully automatic EEG diagnostic system in neonatal intensive care unit (NICU) is the contamination of the EEG by various artifacts in sections of the EEG recording (see illustrative example in Figure 3). These artifacts impede automated neonatal EEG analyses thereby limiting their usefulness to the neonatologist in the NICU. Any automated system that is considered for use in the NICU needs to have a pre-processing stage to detect artifacts.

This study is a contribution towards an overall plan to develop such an automated EEG diagnostics system. In order to develop and deploy such a system in NICUs, there is a need to design the pre-processing artifact detection system as a switch that passes artifact free signal segments to the automated EEG signal classification system but redirects artifact contaminated EEG segments

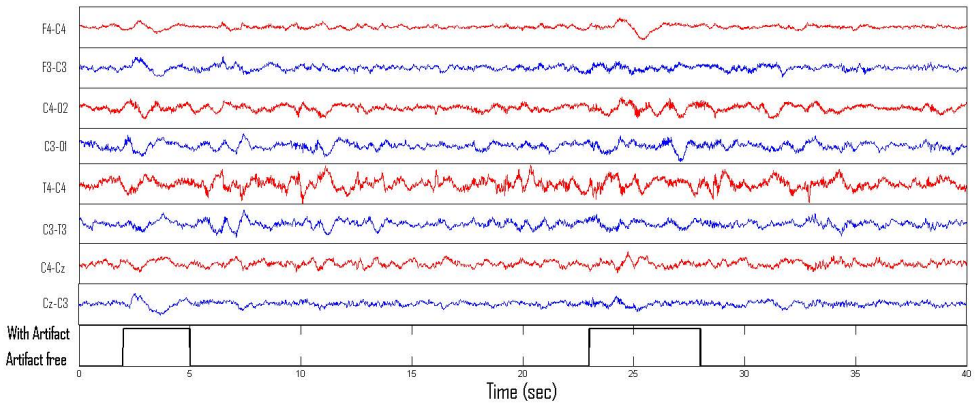

Figure 3: EEG of a newborn contaminated by artifacts. *The plot at the bottom shows the binary mask prepared by a pediatric neurologist.*

to an artifact removal system; the objective being to ensure that artifact free segments are not distorted by unnecessary filtering that can degrade useful information. The overall block diagram is shown in Figure 4. As previously mentioned, a major difficulty with all of the above objectives is that EEG signals are non-stationary [1], with spectral characteristics that change with time, and, therefore require a (t, f) approach, as detailed in Section 3. Note that the 2 stages of artifact removal and abnormality identification are shown only for context, as they are not included in the scope of this contribution.

A large number of methods for artifact detection have been developed in the case of adult EEG signals [15, 16, 17, 18], but these methods cannot be applied to neonatal EEG signals as the latter have much more diversity in their patterns [19]. Previous studies used features based on spectral, temporal, statistical properties and wavelet decomposition to discriminate artifacts from other abnormalities having similar morphologies [19], but the method is not general enough to discriminate all kinds of artifact free signals from with-artifact signals. Instead, this new study assesses the performance of a new set of (t, f) features in discriminating signals corrupted by artifacts from signals free of artifacts without taking into account the underlying characteristics of

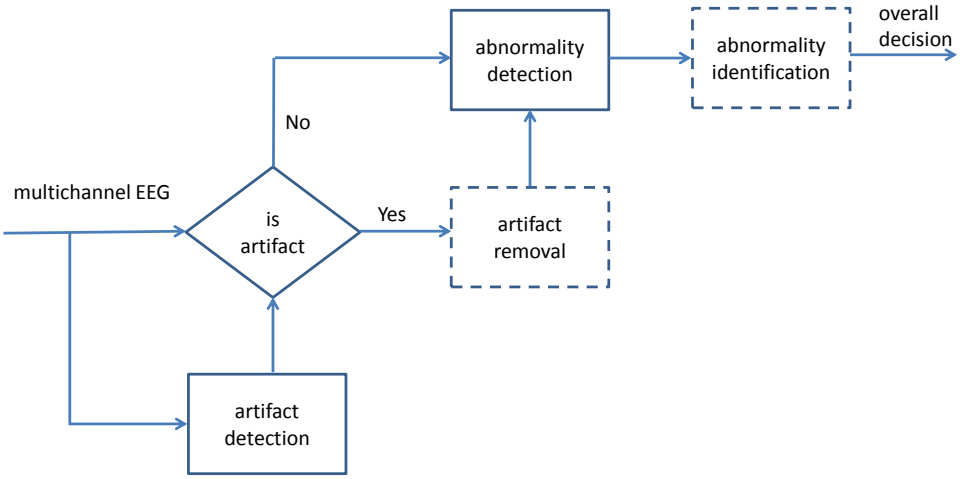

Figure 4: Overall block diagram of an EEG-based automatic diagnostic system. Note that *artifact removal* and *abnormality identification* stages are not part of this contribution.

EEG signals. This is necessary as a pre-processing stage for a refined decision–making in newborn EEG.

3. Automated detection of newborn EEG abnormalities and artifacts using (t, f) features

3.1. Newborn EEG databases

This study used the following two databases.

Database 1 is composed of multichannel EEG signals with 20 channels of continuous EEG recordings collected from 5 newborns admitted to the Royal Brisbane and Women's Hospital, Brisbane, Australia. Fig. 5 shows the arrangement of the 20 electrodes used for acquiring the EEG signals recorded in this study. The channels are labeled as: F4-T4, T4-T6, T6-O2, F3-T3, T3-T5, T5-O1, F4-C4, C4-P4, P4-O2, F3-C3, C3-P3, P3-O1, T4-C4, C4-CZ, CZ-C3, C3-T3, T6-P4, P4-PZ, PZ-P3, and P3-T5. The average recording per subject was 28 minutes. The signals were recorded using bipolar montage, according to the 10-20 standard [20], by a Medelec Profile system (Medelec,

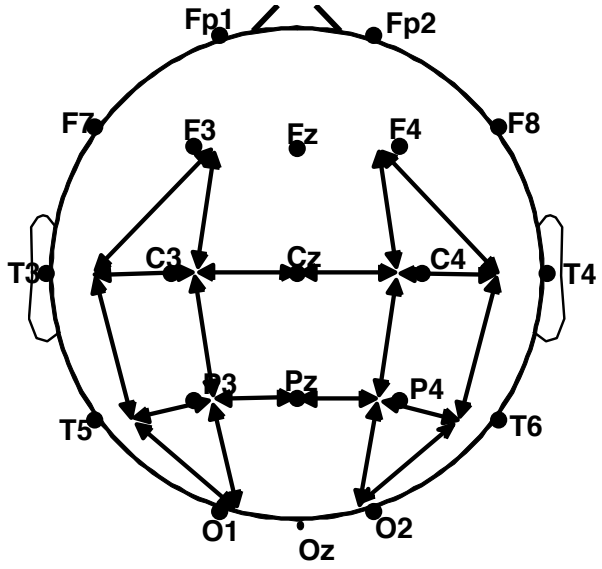

Figure 5: Location and nomenclature of the electrodes on the baby's head. *The circles show the location of the 20 electrodes from which the signals have been recorded.*

Oxford Instruments, Old Woking, UK) at $f_s = 256$ Hz sampling rate. Seizures were marked in the acquired EEG signals by a paediatric neurologist from the Royal Children's Hospital, Brisbane, Australia.

Database 2 consists of one hour long EEG recordings from 39 neonates, acquired at Cork University Maternity Hospital, Ireland for Qatar University as part of a Qatar National Research Foundation (QNRF) funded NPRP project. The EEG data was recorded using the Nicolet One video-EEG. A referential montage of 9 electrodes placed at F3, F4, C3, C4, CZ, T3, T4, O1, and O2 was used to record the EEG (based on the 10-20 International System of Electrode Placement). An 8 channel bipolar montage, i.e. F4-C4, F3-C3, C4-02, C3-01, T4-C4, C3-T3, C4-CZ, and CZ-C3, was formed from these electrodes. The data was recorded with a sampling frequency of 256 Hz; this is followed by bandpass filtering in $(0.5 - 70)$ Hz band with an additional 50 Hz notch filter. The database was marked for artifact by an experienced EEG specialist, with 50% of the artifacts annotated on a channel by channel basis. This database contains artifacts generated

by the movement of subjects, eye blinking, electrocardiogram, respiration, electrode disconnect, interference from the other electrical appliances in NICU, and sweating [21].

3.2. Time-frequency image formation

This study used (t, f) features extracted from the images formed by the quadratic TFD (QTFD) of EEG signals to detect changes in the signals caused by the presence of abnormalities or artifacts. To do this, each EEG segment, i.e. $x[n]$, was first transformed to the (t, f) domain using a QTFD $\rho_{z_x}[n, k]$ which can be expressed as [1]:

$$\rho_{z_x}[n,k] = 2 \underset{m \to k}{\mathrm{DFT}} \left\{ G[n,m] \underset{n}{*} (z_x[n+m] z_x^*[n-m]) \right\} \tag{1}$$

where $z_x[n] = x[n] + \mathcal{H}\{x[n]\}$ and $\mathcal{H}\{\ \}$ stands for the Hilbert transform [3, pp. 13–15]. QTFDs represent a class of methods widely used in practical applications for representing and processing non-stationary signals [1]. In (1), $G[n, m]$ is the time–lag kernel of the TFD and $\underset{n}{*}$ stands for discrete convolution in time. For an N–point signal $x[n]$, $\rho_{z_x}[n, k]$ is represented by an $N \times M$ matrix $\boldsymbol{\rho_{z_x}}$ where M is the number of FFT points used in calculating the TFD. Note that $M = N$ if N is a power of 2; otherwise M is equal to the next power of 2 above N.

Different kernels $G[n, m]$ in (1) allow to define different TFDs, that are most specifically adapted to particular classes of signals [1]. For the analysis of multicomponent signals, such as newborn EEGs, it is often intuitively expected that one needs to use TFDs which reduce the effects of cross–terms while giving a good resolution. These TFDs are known as reduced interference TFDs (RI-TFDs). Five RI-TFDs are considered in this study, namely: modified B–distribution (MBD), Smoothed Wigner–Ville distribution (SWVD), Choi–Williams distribution (CWD), Spectrogram (SPEC), and extended MBD (EMBD) [1, 4]. In addition, the WVD was also used in the comparison

Distribution	$G[n,m]$	**Parameters**
WVD	$\delta[n]$	N/A
SWVD	$\delta[n]w[m]$	$w[n]$:Hamming, $\frac{N}{4}$ samples long
CWD	$\frac{\sqrt{\pi\sigma}}{2\lvert m\rvert}\exp\left(\frac{-\pi^2\sigma n^2}{4m^2}\right)$	$\sigma = 5$
SPEC	$w[n+m]w[n-m]$	$w[n]$:Hamming, $\frac{N}{4}$ samples long
MBD	$\frac{\cosh^{-2\beta}n}{\sum_n \cosh^{-2\beta}n}$	$\beta = 0.01$
EMBD	$\frac{\cosh^{-2\beta}n}{\sum_n \cosh^{-2\beta}n}\frac{\cosh^{-2\alpha}m}{\sum_n \cosh^{-2\alpha}m}$	$\alpha = 0.9,\ \beta = 0.01$

Table 1: The time-lag kernels of the TFDs used in this paper. (*The parameters α, β, and σ are real and positive, N is the length of the signal under analysis, and $w[n]$ represents the window function used in SWVD and SPEC kernels.)*

as it was shown that under some circumstances, the cross–terms caused by the bi–linearity of the WVD can be useful for classification [22]. The expressions for the time–lag kernels $G[n,m]$ of those selected TFDs are listed in Table 1. The parameters of the TFDs given in Table 1 are typical ones for which the TFDs have shown good performances in analyzing EEG signals [1, 3, 4].

3.3. Feature extraction

TFDs are rich in information, but all the (t,f) points cannot be used as features for the classification as that would significantly increase the dimensionality of the problem. In order to avoid this curse of dimensionality, a small representative set of features describing the relevant information for the signal classification must be extracted from TFDs. This section presents first a methodology for defining new (t,f) features by extending t-domain and f-domain features to the joint (t,f) domain. In addition, some additional complementary and inherent (t,f) features are presented for completeness.

3.3.1. Extension of f-domain features to the joint (t, f) domain

Frequency–domain features such as the spectral flux, spectral entropy and spectral flatness are often employed for the detection of abnormalities in biomedical signals [23]. However, these features do not consider the time–varying characteristic of non-stationary signals and may fail to discriminate between two such signals that are different but have similar magnitude spectrum [3, Chapter 1]. For example, the spectral flatness can be used to discriminate between a narrow band signal (e.g. a tone) and a wide band signal (e.g. pure noise or a linear frequency modulated (LFM) signal), but it cannot discriminate between two different wide band signals like an LFM signal and noise occupying the same bandwidth although these two signals have completely different (t, f) signatures. This problem of the above mentioned f-domain features can be overcome by extending them to the (t, f) domain as discussed below.

1. **Extension of spectral flux to (t, f) flux:** The spectral flux measures the rate of change of the spectral content of a signal with time and, by extension, it can be estimated directly from the signal's TFD using [24]:

$$\mathcal{FL}_{(f)} = \sum_{n=1}^{N} \sum_{k=1}^{N} \left| \rho_{z_x}[n+l, k] - \rho_{z_x}[n, k] \right| \tag{2}$$

where l is the time-duration between two slices of a TFD and it can assume any integer value between 1 to $N-1$. This measure can be used to discriminate a signal with slow varying spectral content (e.g. EEG seizure signals with LFM characteristics) from a signal with a fast varying spectral content (e.g. EEG background) as the spectral flux for the former class of signals should be lower compared to the latter class of signals. In this study, $l = N/4$ was chosen in (2).

The spectral flux as defined in (2), has a limitation as for instance, it cannot discriminate EEG seizure signals with spiky characteristics from the EEG background as TFDs of such EEG seizure signals have a sudden variation of the signal energy along the time-axis resulting in a higher spectral flux. In order to measure the variation of the signal energy both along time and along frequency axes, the (t, f) flux is defined as:

$$\mathcal{FL}_{(t,f)} = \sum_{n=1}^{N-l} \sum_{k=1}^{M-m} \Big| \rho_{z_x}[n+l, k+m] - \rho_{z_x}[n, k] \Big| \tag{3}$$

where l and m are predetermined values that depend on the rate of change of the signal energy in the (t, f) plane. They can assume any integer value in between 0 to N-1 and 0 to M-1 respectively. This study used $l = 1$ and $m = 1$ in (3) to calculate the (t, f) flux.

2. **Extension of spectral flatness to (t, f) flatness:** The spectral flatness (SF) measures the level of uniformity of the energy distribution in the f-domain and is defined as the geometric mean of the magnitude spectrum of the signal normalized by its arithmetic mean, i.e. [24]:

$$\mathcal{SF}_{(f)} = M \frac{\left(\prod_{k=1}^{M} \Big| Z_x[k] \Big| \right)^{M^{-1}}}{\sum_{k=1}^{M} \Big| Z_x[k] \Big|} \tag{4}$$

where $Z_x[k]$ is the Fourier transform (FT) of the analytic associate of a real signal $x[n]$ and M is the length of $Z_x[k]$. A maximum value occurs when all values of $Z_x[k]$ are equal. A high value of the SF implies that a signal is wide–band, whereas a low value of the SF implies that a signal is narrow–band. This measure discriminates a pure noise from a tone embedded in noise. However, it cannot detect an LFM signal in noise as the LFM signal is also a wide–band signal just like noise.

TFDs concentrate energy for LFM signals just like the FT concentrates energy for tones. A

feature that measures the flatness of a TFD can therefore be used to detect an LFM signal in noise. For this purpose, the SF is extended to the (t, f) flatness by replacing the geometric and arithmetic means of the FT of a signal in (4) with the geometric and arithmetic means of a TFD. The (t, f) flatness is thus defined as:

$$\mathcal{SF}_{(t,f)} = MN \frac{\prod_{n=1}^{N} \prod_{k=1}^{M} \rho_{z_x}[n,k]}{\sum_{n=1}^{N} \sum_{k=1}^{M} \rho_{z_x}[n,k]}. \tag{5}$$

The (t, f) flatness, for instance, can be used to detect the seizure activity in EEG signals as the energy of EEG seizure signals is usually concentrated in the (t, f) domain along the IFs of the signal components resulting in lower values of the (t, f) flatness, whereas the energy of the EEG background signal is randomly distributed in the (t, f) domain resulting in higher values of the (t, f) flatness. Note that the (t, f) flatness assumes zero value even if there is a single zero in a TFD. So, in practical implementations all zeros of a TFD are replaced by very small values (i.e. epsilon in MATLAB).

3. **Extension of spectral entropy to (t, f) entropy:** The spectral entropy (SE) measures the randomness in the distribution of the signal energy in the f-domain and can be defined as [24]:

$$SE_{(f)} = -\sum_{k=1}^{M} \mathcal{Z}_x[k] \log_2 \mathcal{Z}_x[k] \tag{6}$$

where $\mathcal{Z}_x[k] = \left|Z_x[k]\right|^2 / \left(\sum_k \left|Z_x[k]\right|^2\right)$. High SE implies more randomness or the uniform distribution of the signal energy in a f-domain; while low entropy implies less randomness or more concentration of the signal energy in the f-domain. A simple extension of the SE is

obtained by replacing the FT of the signal in (6) with its normalized TFD, i.e.:

$$SE_{(t,f)} = -\sum_{n=1}^{N}\sum_{k=1}^{M} \frac{\rho_{z_x}[n,k]}{\sum_n \sum_k \rho_{z_x}[n,k]} \log_2 \left(\frac{\rho_{z_x}[n,k]}{\sum_n \sum_k \rho_{z_x}[n,k]} \right) \tag{7}$$

and is known as the (t, f) Shannon entropy [3, Section 7.3]. It measures the randomness of the distribution of the signal energy in a (t, f) domain. A higher value of $SE_{(t,f)}$ implies that the signal energy is uniformly spread in the (t, f) plane while a lower value of $SE_{(t,f)}$ indicates that the signal energy is more concentrated in specific regions in the (t, f) plane. This measure can be used to discriminate between two kinds of wide–band signals such that one class of signals is sparser in the (t, f) plane as compared to the other class; e.g. the energy of EEG seizure signals is more concentrated in the (t, f) domain as compared to the random EEG background.

The (t, f) Shannon entropy has some limitations as it cannot be used for TFDs that can assume negative values. For such TFDs, the (t, f) Renyi entropy and normalized (t, f) Renyi entropy can be used [25]. Here, the normalized (t, f) Renyi entropy is used because of its superior performance in terms of its ability to discriminate EEG seizure signals from the EEG background. It is defined as [3, Section 7.3]:

$$RE_{(t,f)} = \frac{1}{1-\alpha} \log_2 \sum_{n=1}^{N}\sum_{k=1}^{M} \left(\frac{\rho_{z_x}[n,k]}{\sum_n \sum_k \rho_{z_x}[n,k]} \right)^{\alpha} \tag{8}$$

where α is an odd integer and $\alpha > 2$. In this study, we have chosen $\alpha = 3$ [25].

Feature	t**-domain representation**	(t,f) **Extension**
mean	$m_{(t)} = \frac{1}{N}\sum_n x[n]$	$m_{(t,f)} = \frac{1}{NM}\sum_n\sum_k \rho[n,k]$
variance	$\sigma^2_{(t)} = \frac{1}{N}\sum_n (x[n]-m_{(t)})^2$	$\sigma^2_{(t,f)} = \frac{1}{NM}\sum_n\sum_k (\rho_{z_x}[n,k]-m_{(t,f)})^2$
skewness	$\gamma_{(t)} = \frac{1}{N\sigma^3_{(t)}}\sum_n (x[n]-m_{(t)})^3$	$\gamma_{(t,f)} = \frac{1}{(NM-1)\sigma^3_{(t,f)}}\sum_n\sum_k (\rho_{z_x}[n,k]-m_{(t,f)})^3$
kurtosis	$k_{(t)} = \frac{1}{N\sigma^4_{(t)}}\sum_n (x[n]-m_{(t)})^4$	$k_{(t,f)} = \frac{1}{(NM-1)\sigma^4_{(t,f)}}\sum_n\sum_k (\rho_{z_x}[n,k]-m_{(t,f)})^4$
coefficient of variation	$c_{(t)} = \frac{\sigma_{(t)}}{m_{(t)}}$	$c_{(t,f)} = \frac{\sigma_{(t,f)}}{u^{(t,f)}}$

Table 2: Time–frequency extension of t-domain features.

3.3.2. Extension of t-domain features to joint (t,f) domain

Several t-domain features are directly related to the statistical properties of a signal under the assumption that normal and abnormal signals have different probability distributions, implying that the parameters characterizing the probability distributions of normal and abnormal signals can be used as features. A list of statistical features that can be extracted from the t-domain representation is given in Table 2. In order to exploit the additional information provided by TFDs, the t-domain features are extended to the (t,f) features by simply replacing the 1D t-domain moments with the corresponding 2D (t,f) domain moments as illustrated in Table 2. So, in essence, signal characteristics are extended to (t,f) image characteristics.

There are in fact more (t,f) features that can be defined as extensions, including the instantaneous frequency (IF) which is an extension of the mean or central frequency. But as the IF is a function and not a scalar, features based on the IF will be introduced in the next section for clarity and convenience.

3.3.3. Complementary inherent (t, f) features

Some features are inherently (t, f) features; they may not have an obvious direct meaningful counterpart in either t-domain and f-domain. A list of a few such (t, f) features is given below for completeness.

1. **IF-based features** can be derived from the statistics of the IF, i.e. $f_{z_x}[n]$; this includes its mean and its standard deviation, i.e. $\max(f_{z_x}[n]) - \min(f_{z_x}[n])$.

   The IF of a given non–stationary signal describes how its frequency content changes with time [26]. For a mono-component signal $x[n]$, the IF is defined as the derivative of its instantaneous phase (IP) and can be estimated using different methods [27], such as the first order moment of the signal's TFD given by:

$$f_{z_x}[n] = \frac{f_s}{2M} \frac{\sum_{k=1}^{M} k \rho_{z_x}[n,k]}{\sum_{k=1}^{M} \rho_{z_x}[n,k]}. \tag{9}$$

   Note that this feature is included here as complementary although the IF can be interpreted as the extension of the central frequency for non-stationary signals [3, p. 21]; such extension is however a function and not a scalar, and the 1D corresponding feature to the IF standard deviation would be meaningless.

2. **Matrix decomposition based features** are obtained from a decomposition of the TFD matrix $\boldsymbol{\rho_{z_x}}$. This study uses two matrix decomposition methods, namely: singular value decomposition (SVD) and non-negative matrix factorization (NMF) [28, 29]. Such methods have proved useful in characterizing non-stationary signals [28, 30, 31].

   (a) **SVD** can be performed on the $N \times M$ matrix $\boldsymbol{\rho_{z_x}}$. It divides the TFD matrix into two subspaces, signal subspace and an orthogonal alternate subspace of the form given

below in (10).

$$\boldsymbol{\rho_{z_x}} = \boldsymbol{USV^H} \tag{10}$$

where $\boldsymbol{U}$ is an $N \times N$ real matrix, $\boldsymbol{S}$ is an $N \times M$ diagonal matrix with non-negative real numbers $(s_i, i = 1, 2, \cdots, N)$ on the diagonal, and $\boldsymbol{V^H}$ (the conjugate transpose of $\boldsymbol{V}$ is an $M \times M$ real unitary matrix. The diagonal entries of $\boldsymbol{S}$ are known as the singular values of $\boldsymbol{\rho_{z_x}}$. SVD-based features are extracted from the singular values of the matrix $\boldsymbol{\rho_{z_x}}$. This includes, for example, the maximum of the singular values which can be chosen as characteristic features of the singular values of $\boldsymbol{\rho_{z_x}}$. Another possible feature is the (t, f) complexity measure estimated from the Shannon entropy of the singular values of the matrix $\boldsymbol{\rho_{z_x}}$. It represents the magnitude and number of non-zero singular values of a TFD and is given by:

$$CM = -\sum_{i=1}^{N} \bar{s_i} \log_2 \bar{s_i} \tag{11}$$

where $\bar{s_i}, i = 1, 2, \cdots, N$ are the normalized singular values of the matrix $\boldsymbol{\rho_{z_x}}$, i.e. $\bar{s_i} = s_i / \sum_i s_i$.

(b) **NMF** is another matrix decomposition technique which can be used to extract features from TFDs. It has the advantage of preserving the non-negativity of the entries which is important to obtain meaningful physical interpretation under some circumstances. Moreover, the resulting matrices have lower dimensions and thus provide a less complex characterization of the original matrix [32].

The NMF factorizes a given non-negative matrix into two non-negative matrices as

follows [32]:

$$\boldsymbol{\rho}_{\boldsymbol{z_x}} \approx \boldsymbol{W}\boldsymbol{H} = \sum_{r=1}^{R} w_r h_r \tag{12}$$

where the columns of the matrices $\boldsymbol{W}$ $(N \times R)$ and $\boldsymbol{H}$ $(R \times M)$ are known as base and coefficient vectors, respectively, and R $(R \ll min(M, N))$ is the decomposition parameter and is usually application–dependent. The base vectors, i.e. $w_r, r = 1, ..., R$, can be interpreted as characteristic frequency structures whereas the coefficient vectors, i.e. $h_r, r = 1, ..., R$, can be regarded as the temporal location of these structures [31]. Based on the decomposition in (12), the sparsity of the base and coefficient vectors can be defined respectively as:

$$S_{w_r} = \frac{1}{\sqrt{N}} \left(\sqrt{N} - \frac{\sum_{l=1}^{N} w_r(l)}{\sqrt{\sum_{l=1}^{N} w_r^2(l)}} \right), \ r = 1, ..., R \tag{13}$$

$$S_{h_r} = \frac{1}{\sqrt{M}} \left(\sqrt{M} - \frac{\sum_{l=1}^{M} h_r(l)}{\sqrt{\sum_{l=1}^{M} h_r^2(l)}} \right), \ r = 1, ..., R \tag{14}$$

Different statistics of S_{w_r} and S_{h_r} such as their means and standard deviations (std) can then be considered as NMF-based features.

3. **TFD concentration measure** determines the concentration of the signal's representation in the (t, f) domain [33]. Here, we use the definition given in [34] as it does not discriminate between low concentrated components and highly concentrated ones. It is given by:

$$\mathcal{M} = \left(\sum_{n=1}^{N} \sum_{k=1}^{M} |\rho_{z_x}[n, k]|^{\frac{1}{2}} \right)^2. \tag{15}$$

Note that the signals with power distributed all over the (t, f) plane have a larger $\mathcal{M}$, while

class	feature name	formula
extended f-domain features; see eqs. (3), (5) and (8)	(t,f) flux	$TF_1 = \mathcal{FL}_{(t,f)}$
	(t,f) flatness	$TF_2 = \mathcal{SF}_{(t,f)}$
	Renyi entopy	$TF_3 = RE_{(t,f)}$
extended t-domain features; see Table 2	mean	$TF_4 = m_{(t,f)}$
	variance	$TF_5 = \sigma^2_{(t,f)}$
	skewness	$TF_6 = \gamma_{(t,f)}$
	kurtosis	$TF_7 = k_{(t,f)}$
	coefficient of variation	$TF_8 = c_{(t,f)}$
complementary (t,f) features; see eqs. (9), (11), (13), (14), and (15)	mean of the IF	$TF_9 = \frac{1}{N}\sum_{n=1}^{N} f_{z_x}[n]$
	deviation of the IF	$TF_{10} = \max\left(f_{z_x}[n]\right) - \min(f_{z_x}[n])$
	maximum of singular values	$TF_{11} = \max(\bar{s_1}, ..., \bar{s_N})$
	complexity measure	$TF_{12} = CM$
	mean of S_{w_r}	$TF_{13} = \frac{1}{R}\sum_{r=1}^{R} S_{w_r}$
	standard deviation of S_{w_r}	$TF_{14} = \mathrm{std}(S_{w_1}, ..., S_{w_r})$
	mean of S_{h_r}	$TF_{15} = \frac{1}{R}\sum_{r=1}^{R} S_{h_r}$
	standard deviation of S_{h_r}	$TF_{16} = \mathrm{std}(S_{h_1}, ..., S_{h_r})$
	TFD concentration measure	$TF_{17} = \mathcal{M}$

Table 3: Time–frequency features used for automatic detection of artifacts and seizures in newborn EEG signals; (TF_i is the i^{th} (t,f) feature, $f_{z_x}[n]$ *is the IF of* $x[n]$, $\bar{S_1}, ..., \bar{S_N}$ *are the normalized singular values of the matrix* $\boldsymbol{\rho_{z_x}}$, *and* S_{w_r} *and* S_{h_r} *are the sparsity of the base and coefficient vectors of* $\boldsymbol{\rho_{z_x}}$, *respectively).*

those with power concentrated in certain areas are characterized by a smaller $\mathcal{M}$. This feature is also included in this section for convenience although it could be interpreted as an extension of a f-domain feature.

3.4. Selected features

Among the (t,f) features presented in Section 3.3, a selected subset of features is listed in Table 3. In order to compare their performance with their t-domain and f-domain features counterparts, and answer the main research question, the features listed in Table 4 were also extracted.

3.5. Implementation

From an EEG segment $x[n]$, the (t,f) features listed in Table 3 were extracted from the TFD $\rho_{z_x}[n,k]$. The TFDs were calculated using (1) with the kernels listed in Table 1. The IF of $x[n]$ was estimated using the first order moment of its TFD $\rho_{z_x}[n,k]$ (see (9)). Also, to decompose

class	feature name	formula
f-domain features; see eqs. (2), (4) and (6)	spectral flux	$F_1 = \mathcal{FL}_{(f)}$
	spectral flatness	$F_2 = \mathcal{SF}_{(f)}$
	spectral entropy	$F_3 = SE_{(f)}$
t-domain features; see Table 2	mean	$T_1 = m_{(t)}$
	variance	$T_2 = \sigma^2_{(t)}$
	skewness	$T_3 = \gamma_{(t)}$
	kurtosis	$T_4 = k_{(t)}$
	coefficient of variation	$T_5 = c_{(t)}$

Table 4: t-domain and f-domain features used for automatic detection of artifacts and seizures in newborn EEG signals; (T_i and F_i are the i^{th} t-domain and f-domain features, respectively).

the TFD matrices, we used an NMF approximation based on alternating non-negative constrained least squares and active set method, as it has been shown to have superior performance in terms of convergence and implementation [29]. The factorization uses an iterative method and, because the objective function often has local minima, repeated factorizations may yield different W and H matrices. The study showed that in most cases the algorithm converges to solutions of rank lower than $R = 16$. This value was the used for extracting NMF-based features. Note that the decomposition of $\rho_{z_x}[n, k]$ using the NMF requires the matrix to be non-negative, which is not the case for the TFDs listed in Table 1 except the SPEC. We therefore defined this feature by assigning zero to the negative values in $\rho_{z_x}[n, k]$ before implementing the NMF algorithm.

The t-domain and f-domain features listed in Table 4 were extracted from $x[n]$ and $Z_x[k]$ (i.e. the FT of its analytic associate), respectively.

3.6. Performance evaluation

3.6.1. ROC analysis

The performance of each feature in detecting seizures and artifacts in newborn EEG was evaluated by performing a ROC analysis on the values of the feature extracted from EEG segments belonging to different states (e.g. seizure and non-seizure). For a given feature, the ROC curve of

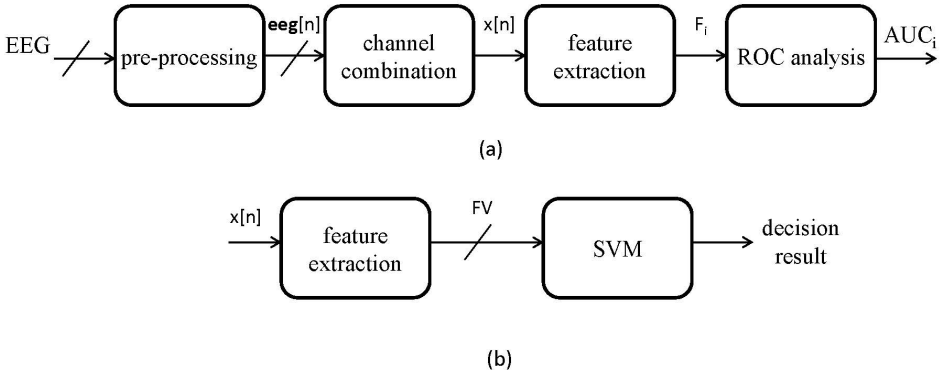

Figure 6: (a) The methodology for evaluating the performance of (t, f) features for detecting seizures in newborn EEG. For each feature, the ROC analysis is performed and the resulting AUC is used as the performance measure. (b) A SVM uses a vector containing the selected (t, f) features to detect an abnormal segment.

a binary classifier based on that feature was estimated as its discrimination threshold was varied. The area under the resulting ROC, i.e. AUC, was computed and used as a summary of the ROC curve and a measure of how well a feature can discriminate between two groups. All the simulations were carried out in MATLAB. The implementations of QTFDs were obtained from the TFSA toolbox [35], available at: www.time-frequency.net (also available on Qatar University Qspace or The University of Queensland Espace).

3.6.1.1. Seizure detection.

Figure 6(a) shows the methodology used in this study for evaluating the performance of (t, f) features in detecting changes in newborn EEG signals caused by the presence of seizures using the AUC as the performance criteria. The EEG signals in **Database 1** (discussed in Section 3.1) were first inspected visually by an EEG expert to remove highly artifactual segments. At the pre-processing stage, the signals were band–pass filtered in $(0.5 - 16)$ Hz (given that neonatal EEG seizures have been reported to have spectral activities mostly below 12 Hz [36, 37]) and down–sampled at 32 Hz (to reduce computational load).

For detecting seizures in newborn EEGs, the signals were combined into one signal by space

averaging over the various channels using:

$$x[n] = \frac{1}{20}\sum_{i=1}^{20} \mathrm{eeg}_i[n]\cdot \tag{16}$$

in order to improve their SNR and enhance the signatures of abnormalities in the (t, f) domain [13], given that the question of localization was not considered in this study. A selection of 80 non-overlapping seizure segments and 80 non-overlapping non-seizure segments of length 8 seconds were extracted randomly from 27 min of artifact–free seizure signals and 39 min of artifact–free non-seizure signals.

3.6.1.2. Artifact detection.

The EEG signals in **Database 2** (discussed in Section 3.1) were processed to extract 20 000 single channel artifact free segments and the same amount of segments contaminated with artifacts from EEG signals. Each segment has one second duration, as it is the minimum duration of an artifact in the given database. The selection of one second for the duration of the EEG segments for artifact detection is also supported by previous studies, e.g. [38, 39, 40].

3.6.2. Classification

In order to evaluate the performance of the (t, f) features and compare it with t- and f-domains features, three feature vectors: $FV_1 = \{F_i\}_{i=1}^{3} \cup \{T_i\}_{i=1}^{5}$ (composed of t- and f-domains features), $FV_2 = \{TF_i\}_{i=1}^{8}$ (composed of the extended t- and f-domains features), and $FV_3 = \{TF_i\}_{i=9}^{17}$ (composed of the complementary (t, f) features) were used to train three support vector machines (SVMs); see Figure 6(b). The features are presented in Tables 3 and 4. The selection of SVMs is motivated by the fact that they have proven to be well suited for EEG abnormality detection [41, 42]. The output of the SVM shows the decision taken, e.g. whether the EEG signal $x[n]$ is a

seizure or non-seizure.

We used SVMs with radial basis function kernels with scaling factor of 1 to evaluate the overall detection performance of the features listed in Tables 3 and 4. The performance of the proposed methodology was evaluated using the standard statistical parameters of the SVM, i.e. its sensitivity (SEN), specificity (SPE), positive predictive value (PPV), negative predictive value (NPV), and total accuracy (ACC). These quantities are defined below.

$$\text{SEN} = \frac{number\,of\,true\,positives}{number\,of\,true\,positives\;+\;number\,of\,false\,negatives} \tag{17a}$$

$$\text{SPE} = \frac{number\,of\,true\,negatives}{number\,of\,true\,negatives\;+\;number\,of\,false\,positives} \tag{17b}$$

$$\text{PPV} = \frac{number\,of\,true\,positives}{number\,of\,true\,negatives\;+\;number\,of\,false\,positives} \tag{17c}$$

$$\text{NPV} = \frac{number\,of\,true\,negatives}{number\,of\,true\,negatives\;+\;number\,of\,false\,negatives} \tag{17d}$$

$$\text{ACC} = \frac{number\,of\,true\,positives\;+\;number\,of\,true\,negatives}{number\,of\,positives\;+\;number\,of\,negatives} \tag{17e}$$

For the artifact detection experiment, these quality measures were estimated using 10-fold cross–validation such that the entire database was divided in 10 equal sets. Out of 10 sets, 9 sets are used for training while 1 set is used for testing. This process is repeated 10 times such that each set is tested once. The final results are obtained by averaging the results of all the iterations. In the

seizure detection experiment, due to the relatively small size of the database used, a leave–one–out cross–validation was used to evaluate the performance of the classifiers.

4. Results and discussions

4.1. Performance evaluation of features using ROC analysis

4.1.1. Seizure detection

All the features listed in Tables 3 and 4 were then extracted from the TFD of $x[n]$. For each feature, a ROC analysis was performed and its AUC was calculated. Table 5 shows the AUC values for the features extracted from different TFDs. A Student's t-test was also used to assess the statistical significance of improvement obtained as a result of extending t-domain or f-domain features to the joint (t, f) domain and the resulting p-values for (t, f) extended features are shown inside brackets.

The results show that among different (t, f) features listed in Table 3, the feature TF_{13}, i.e. the average of the base vectors of $\boldsymbol{\rho}_{\boldsymbol{z}_x}$ extracted from the SWVD, outperforms other features. We also observe that most of the extended (t, f) features have better performance than their t-domain or f-domain counterparts. For illustration, box plots of the (t, f) features TF_1 and TF_6 and their t-domain or f-domain counterparts (i.e. F_1 and T_3, respectively) for seizure and non-seizure segments, are shown in Fig. 7. (See Tables 3 and 4 also). The plots show clearly that the (t, f) features allow for better discrimination between the two classes.

The AUC scores in Table 5 also imply that the selection of the best performing (t, f) features depends on the type of TFD used for representing the signal $x[n]$ in the (t, f) domain. For example, if one chooses the SWVD for transforming the signal to the (t, f) domain, then the features TF_8, TF_9, and TF_{13} are the best performing ones with AUCs$\geq$0.92. The results also suggest that some

(t,f) feature, see Table 3	TFD						original t- or f-domain feature, see Table 4
	WVD	SWVD	CWD	SPEC	MBD	EMBD	
TF_1	0.67(0.02)	0.64(0.06)	0.70(0.01)	0.67(0.02)	0.65(0.04)	0.73(0.00)	0.54 (F_1)
TF_2	0.67(0.02)	0.67(0.02)	0.71(0.00)	0.74(0.00)	0.62(0.10)	0.60(0.17)	0.54 (F_2)
TF_3	0.79(0.00)	0.85(0.10)	0.80(0.01)	0.85(0.10)	0.88(0.30)	0.52(0.00)	0.90 (F_3)
TF_4	0.66(0.02)	0.66(0.02)	0.66(0.02)	0.66(0.02)	0.66(0.02)	0.66(0.02)	0.53 (T_1)
TF_5	0.64(0.37)	0.62(0.26)	0.61(0.21)	0.61(0.21)	0.62(0.26)	0.60(0.17)	0.66 (T_2)
TF_6	0.79(0.00)	0.75(0.00)	0.75(0.00)	0.80(0.00)	0.80(0.00)	0.52(0.44)	0.53 (T_3)
TF_7	0.79(0.01)	0.78(0.01)	0.77(0.02)	0.79(0.01)	0.79(0.01)	0.51(0.01)	0.65 (T_4)
TF_8	0.73(0.00)	0.92(0.00)	0.83(0.00)	0.86(0.00)	0.92(0.00)	0.52(0.44)	0.51 (T_5)
TF_9	0.52	0.92	0.62	0.70	0.83	0.59	
TF_{10}	0.51	0.53	0.51	0.57	0.52	0.52	
TF_{11}	0.57	0.55	0.57	0.59	0.55	0.60	
TF_{12}	0.64	0.78	0.83	0.83	0.79	0.83	
TF_{13}	0.89	0.93	0.91	0.90	0.93	0.89	N/A
TF_{14}	0.51	0.53	0.68	0.53	0.52	0.58	
TF_{15}	0.60	0.79	0.83	0.85	0.83	0.83	
TF_{16}	0.54	0.79	0.55	0.69	0.62	0.62	
TF_{17}	0.64	0.54	0.59	0.59	0.57	0.61	

Table 5: Result of the ROC analysis of the (t,f), t-domain, and f-domain features for the detection of seizures in newborn EEG signals. *The p-values shown inside brackets are obtained from statistical t-test performed to assess the statistical significance of improvement achieved in AUC of features as a result of translating t-only or f-only features to the joint (t,f) domain.*

features, e.g. TF_{10} (deviation of the IF), fail to show the changes in the signal characteristics and therefore should not be used in this application, as by definition, it is not a highly discriminating feature.

4.1.2. Artifact detection

In order to compare the performance of the (t,f) extended features with t-only and f-only features for the detection of artifacts in newborn EEG signals, the method analyzed the extracted segments using the TFDs listed in Table 1. The AUC criterion was used to evaluate the performance

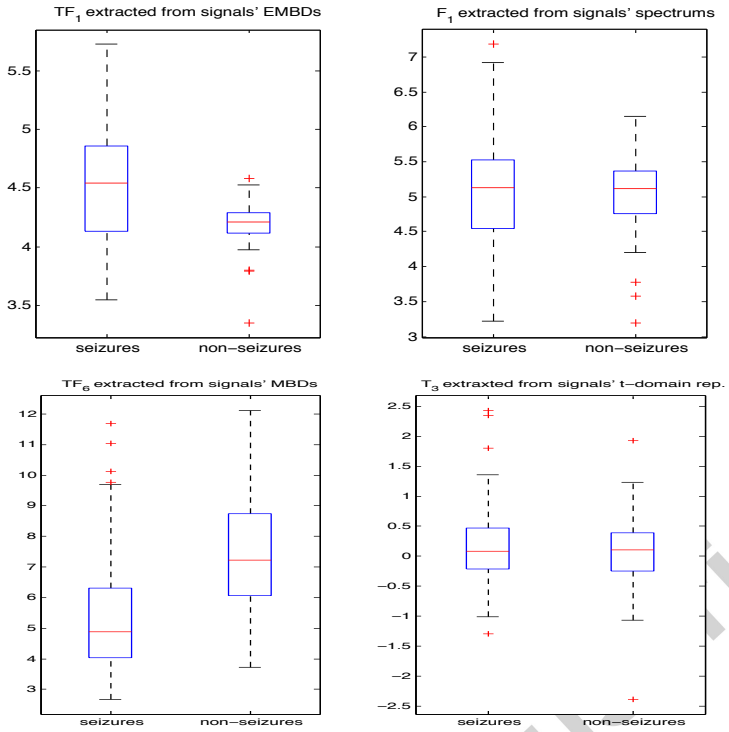

Figure 7: Box plots of four selected features showing the improvement in the discrimination between seizure and non-seizure segments due to the use of the extended t-domain and f-domain features. Top (left) TF_1 extracted from the EMBD and (right) F_1 extracted from the signal's spectrum for seizure and non-seizure segments, bottom (left) TF_6 extracted from the MBD and (right) T_3 extracted from the signal's t-domain representation for seizure and non-seizure segments. Note that TF_1 is the extended version of F_1 and TF_6 is the extended version of T_3. *(On each box, the central mark is the median, the edges are the* 25^{th} *and* 75^{th} *percentiles and whiskers extend to the most extreme data points the algorithm considers to be not outliers. Outliers are represented individually by +.)*

of all the features. The AUC value for the extracted features are given in Table 6.

The results indicate that (t, f) extended features give better performance as compared to the corresponding t-domain or f-domain features. A Student's t-test is also applied to assess the statistical significance of the AUC improvement obtained as a result of extending t-domain or f-domain features to the joint (t, f) domain [42]. The resulting p-values for the (t, f) extended features are shown inside brackets. The experimental results indicate that in most cases, p-values are less than 0.05 which indicates that the improvement in the AUC vales is statistically significant (see e.g. features TF_5 and TF_6). The results also indicate that the best features come from some of the complementary (t, f) features such as TF_9 and TF_{14} which are inherently (t, f) features

(t,f) **feature**, see Table 3	**TFD** WVD	SWVD	CWD	SPEC	MBD	EMBD	original t- or f-domain feature, see Table 4
TF_1	0.51(0.00)	0.51(0.00)	0.51(0.00)	0.51(0.00)	0.51(0.02)	0.51(0.02)	0.50(F_1)
TF_2	0.52(0.00)	0.51(0.02)	0.51(0.02)	0.50(1)	0.51(0.02)	0.50(1)	0.50 (F_2)
TF_3	0.53(0.00)	0.56(0.00)	0.55(0.00)	0.55(0.00)	0.56(0.00)	0.53(0.00)	0.50 (F_3)
TF_4	0.51(1)	0.51(1)	0.51(1)	0.51(1)	0.51(1)	0.51(1)	0.51 (T_1)
TF_5	0.54(0.00)	0.54(0.00)	0.54(0.00)	0.54(0.00)	0.54(0.00)	0.54(0.00)	0.51 (T_2)
TF_6	0.55(0.02)	0.55(0.02)	0.55(0.02)	0.55(0.02)	0.55(0.02)	0.55(0.02)	0.54 (T_3)
TF_7	0.55(0.02)	0.55(0.02)	0.55(0.02)	0.55(0.02)	0.55(0.02)	0.55(0.02)	0.54 (T_4)
TF_8	0.51(0.02)	0.51(0.02)	0.50(1)	0.51(0.02)	0.51(0.02)	0.51(0.02)	0.50 (T_5)
TF_9	0.51	0.52	0.52	0.52	0.52	0.72	
TF_{10}	0.54	0.51	0.51	0.51	0.51	0.51	
TF_{11}	0.51	0.51	0.51	0.51	0.51	0.51	
TF_{12}	0.54	0.50	0.50	0.51	0.50	0.51	
TF_{13}	0.55	0.56	0.56	0.56	0.56	0.56	N/A
TF_{14}	0.50	0.63	0.62	0.62	0.63	0.61	
TF_{15}	0.52	0.56	0.56	0.56	0.56	0.56	
TF_{16}	0.53	0.60	0.61	0.61	0.56	0.60	
TF_{17}	0.51	0.53	0.53	0.53	0.53	0.53	

Table 6: Result of the ROC analysis of the (t,f), t-domain, and f-domain features for the detection of artifacts in newborn EEG signals. *The p-values shown inside brackets are obtained from statistical t-test performed to assess the statistical significance of improvement achieved in AUC of features as a result of translating t-only or f-only features to the joint (t,f) domain.*

and do not have an obvious direct and meaningful correspondent t-only or f-only feature. This improved performance appears to result from the ability of TFDs to better take into account the non-stationary nature of EEG signals. It is however noted that both (t,f) extended features and their t-only or f-only counterparts fail to give good performance. This may be explained by the large variability in type of artifacts. These results are sufficiently encouraging to warrant further research in this area.

4.2. SVM-based decision making

4.2.1. Seizure detection

Table 7 shows the values of the statistical parameters of the SVM-based detector used for detecting newborn EEG seizures for the different feature vectors listed in Table 7 and for different TFDs. The results obtained indicate that the SVM which uses the combined feature vector FV_1 composed of the t- and f-domains features, has a total accuracy of 86.88%. This is mainly due to the presence of the signal power and its spectral entropy (i.e. T_2 and F_3 respectively) in the feature vector; the features which are very discriminative between seizure and non-seizure classes [44]. But, as expected, the use of the combined (t, f) feature set FV_2 composed of the extended t-domain and f-domain features results in a better performance (up to 7% higher total accuracy) compared to FV_1. The results also indicate that the best performing classifier shows a total accuracy of 93.75% and high SEN and SPE, and it uses the (t, f) feature vector FV_2 extracted from the SWVD of EEG signals. On the other hand, we observe that the performance of the classifier which uses FV_2 extracted from the EMBD of EEG signals is much lower than that of the one which uses FV_1. This suggests the need for a data–adapted TFD kernel selection and optimization of its parameters to the dataset.

In addition, t-tests were performed on the values of the classifiers' total accuracies for different subjects to test the statistical significance of the improvement achieved as a result of using (t, f) features instead of t-only or f-only features. The high scores for the resulting p-values, even when the total accuracies are very different, is due to the fact that the size of the database is not large enough (i.e. only 5 subjects) to allow the null hypothesis to be rejected at the 0.05 level.

feature vector	TFD	SVM statistical parameters (%) SEN	SPE	PPV	NPV	ACC
t- and f-domains features, $FV_1 = \{F_i\}_{i=1}^{3} \cup \{T_i\}_{i=1}^{5}$	N/A	92.50	81.25	85.07	92.58	86.88
(t, f) extended t- and f-domains features, $FV_2 = \{TF_i\}_{i=1}^{8}$	WVD	83.75	92.50	92.50	86.35	88.13(0.7608)
	SWVD	95.00	92.50	93.24	95.19	93.75(0.0551)
	CWD	86.25	97.50	97.57	89.30	91.88(0.2701)
	SPEC	86.25	95.00	95.42	89.42	90.63(0.4169)
	MBD	91.25	91.25	92.09	92.06	91.25(0.1995)
	EMBD	57.50	76.25	66.77	67.62	66.88(0.0344)
complementary (t, f) features, $FV_3 = \{TF_i\}_{i=9}^{17}$	WVD	86.25	83.75	84.23	87.93	85.00
	SWVD	93.75	90.00	91.67	94.62	91.88
	CWD	95.00	90.00	91.46	95.67	92.50
	SPEC	93.75	92.50	92.92	94.09	93.13
	MBD	93.75	87.50	89.68	94.62	90.63
	EMBD	98.75	76.25	82.02	98.33	87.50

Table 7: Newborn EEG seizure detection results using SVMs trained with the (t, f), t-domain, and f-domain features (see Tables 3 and 4 for the list of features). *The p-values shown inside brackets are obtained from statistical t-test performed to assess the statistical significance of improvement achieved in the total accuracy of SVM based classifier when the feature vector composed of (t, f) extended features is used instead of feature vector composed of t-only or f-only features.*

4.2.2. Artifact detection

Table 8 shows the artifact detection results of the SVM-based detector trained with the set of (t, f) extended features and the combined set of the corresponding t-only and f-only features. The results indicate that the SVM trained using (t, f) features give better classification performance as compared to the SVM trained using the combined set of the corresponding t-domain and f-domain features; e.g. the set of non (t, f) features using SVM classifier achieves the total accuracy of 65.68%, whereas the (t, f) features extracted from the WVD achieve the total accuracy of 70.85%. A Student's t-test was performed to test the statistical significance of the improvement in total accuracy obtained as a result of using (t, f) features instead of t-only or f-only features [43]. The resulting p-values, shown in brackets, indicate that, except for the features extracted from the SPEC and SWVD, the improvement achieved in the overall performance is in general statistically significant.

feature vector	TFD	SVM statistical parameters (%) SEN	SPE	PPV	NPV	ACC
t- and f-domains features, $FV_1 = \{F_i\}_{i=1}^{3} \cup \{T_i\}_{i=1}^{5}$	N/A	54.49	76.87	70.22	66.93	65.68
(t,f) extended t- and f-domains features, $FV_2 = \{TF_i\}_{i=1}^{8}$	WVD	53.53	88.18	81.94	70.86	70.85(0.0010)
	SWVD	57.02	76.58	70.91	70.00	66.80(0.3072)
	CWD	52.33	87.92	81.24	70.12	70.12(0.0014)
	SPEC	55.09	78.57	72.04	69.35	66.83(0.2705)
	MBD	51.88	87.09	80.07	69.66	69.49(0.0018)
	EMBD	54.38	86.76	80.41	71.01	70.57(0.0013)
complementary (t,f) features, $FV_3 = \{TF_i\}_{i=9}^{17}$	WVD	54.89	78.28	71.62	70.50	66.58
	SWVD	48.38	77.56	68.36	66.40	62.97
	CWD	53.65	77.04	70.01	69.36	65.34
	SPEC	51.21	77.34	69.32	67.99	64.28
	MBD	51.40	78.28	70.31	68.18	64.84
	EMBD	58.04	81.49	75.82	73.14	69.76

Table 8: Newborn EEG artifact detection results using SVMs trained with the (t,f), t-domain, and f-domain features (see Tables 3 and 4 for the list of features). *The p-values shown inside brackets are obtained from statistical t-test performed to assess the statistical significance of improvement achieved in the total accuracy of SVM based classifier when the feature vector composed of (t,f) extended features is used instead of feature vector composed of t-only or f-only features.*

5. Conclusions

The importance of detecting changes in newborn EEG signals can be a matter of life and death, or, a life with a major handicap. The same situation occurs in many other applications (nuclear plants fault detection, tsunami early warning systems, etc) where a change could be catastrophic if not detected early enough. This paper presents a methodology for identifying such changes in an objective manner, taking into account the non-stationary characteristic of such signals. The approach to abnormal change detection involves the extraction and selection of features observed in the (t,f) domain. For this purpose, a methodology was defined that extends time only features and frequency only features to new (t,f) features.

A ROC analysis was used for the performance evaluation of the (t,f) features selected for the detection of changes in EEG signals, caused by abnormalities and artifacts. The results obtained indicate that generally, the (t,f) extended features give better results for the detection of seizures

and artifacts in EEG signals as compared to the corresponding time-only or frequency-only features. Also, the EEG seizure detection results using SVM-based classifiers show that the use of the feature vector composed of the extended t- and f-domains features can result in 7% improvement compared to the feature vector composed of only t-domain and f-domain features. An improvement of 5% in terms of the total accuracy of the artifact detection algorithm is obtained when the feature vector composed of (t, f) extended features is used instead of the feature vector composed of time-only and frequency-only features.

For a particular application, the performance of (t, f) features depends on the type of TFD and no single TFD is the best for the extraction of all (t, f) features. This suggests that a more refined approach for (t, f) based change detection could be adopted where a separate TFD may be used to extract each feature. The computational load of this approach can be significantly reduced by using more computationally efficient algorithms for implementing TFDs (e.g. [1]). In addition, it may be possible to further improve detection results by optimizing the parameters of TFD kernels directly for classification instead of focusing on (t, f) resolution.

Acknowledgments

This work was funded by Qatar National Research Fund, Grant No. NPRP 6-885-2-364 and Grant No. NPRP 4-1303-2-517. The authors would also like to thank Prof. Paul Colditz for providing the EEG abnormality database as part of the above grants, Dr. Ervin Sejdic for commenting the draft submission and the anonymous reviewers for their valuable feedbacks on the manuscript.

References

References

[1] B. Boashash, G. Azemi, and J.M. O' Toole, "Time-frequency processing of nonstationary signals: Advanced TFD design to aid diagnosis with highlights from medical applications", *IEEE Signal Processing Magazine*, vol. 30, no. 6, pp. 108–119, 2013.

[2] R.J. Radke, S. Andra, O. Al-Kofahi, and B. Roysam, "Image change detection algorithms: a systematic survey", *IEEE Transactions on Image Processing*, vol. 14, no. 3, pp. 294–307, 2005.

[3] B. Boashash, Ed., *Time–Frequency Signal Analysis and Processing: A Comprehensive Reference*, Elsevier, Oxford, UK, 2003.

[4] B. Boashash and T. Ben-Jabeur, "Design of a high-resolution separable-kernel quadratic TFD for improving newborn health outcomes using fetal movement detection", in *11th International Conference on Information Science, Signal Processing and their Applications (ISSPA)*, July 2012, pp. 354 –359.

[5] J.J. Volpe, *Neurology of the Newborn*, vol. 899, Elsevier Health Sciences, 2008.

[6] M.A. Navakatikyan, P.B. Colditz, C.J. Burke, T.E. Inder, J. Richmond, and C.E. Williams, "Seizure detection algorithm for neonates based on wave-sequence analysis", *Clinical Neurophysiology*, vol. 117, no. 6, pp. 1190 – 1203, 2006.

[7] R. Hopfengrtner, F. Kerling, V. Bauer, and H. Stefan, "An efficient, robust and fast method for the offline detection of epileptic seizures in long-term scalp EEG recordings.", *Clinical Neurophysiology*, vol. 118, no. 11, pp. 2332–2343, 2007.

[8] K.M. Kelly, D.S. Shiau, R.T. Kern, J.H. Chien, M.C.K. Yang, K.A. Yandora, J.P. Valeriano, J.J. Halford, and J.C. Sackellares, "Assessment of a scalp EEG-based automated seizure detection system", *Clinical Neurophysiology*, vol. 121, no. 11, pp. 1832–1843, 2010.

[9] A. Subasi, E. Erelebi, A. Alkan, and E. Koklukaya, "Comparison of subspace-based methods with AR parametric methods in epileptic seizure detection", *Computers in Biology and Medicine*, vol. 36, no. 2, pp. 195 – 208, 2006.

[10] S. Altunay, Z. Telatar, and O. Erogul, "Epileptic EEG detection using the linear prediction error energy", *Expert Systems with Applications*, vol. 37, no. 8, pp. 5661 – 5665, 2010.

[11] N.F. Güler, E.D. Übeyli, and I.Güler, "Recurrent neural networks employing Lyapunov exponents for EEG signals classification", *Expert Systems with Applications*, vol. 29, no. 3, pp. 506 – 514, 2005.

[12] J.M. O' Toole and B. Boashash, "Time-frequency detection of slowly varying periodic signals with harmonics: Methods and performance evaluation", *EURASIP Journal on Advances in Signal Processing*, vol. 2011, 2011.

[13] M.S. Khlif, P.B. Colditz, and B. Boashash, "Effective implementation of timefrequency matched filter with adapted pre and postprocessing for data-dependent detection of newborn seizures", *Medical Engineering & Physics*, vol. 35, no. 12, pp. 1762 – 1769, 2013.

[14] A.T. Tzallas, M.G. Tsipouras, and D.I. Fotiadis, "Epileptic seizure detection in EEGs using time–frequency analysis", *IEEE Transactions on Information Technology in Biomedicine*, vol. 13, no. 5, pp. 703 –710, Sep. 2009.

[15] A. Delorme, T. Sejnowski, and S. Makeig, "Enhanced detection of artifacts in EEG data using higher-order statistics and independent component analysis", *NeuroImage*, vol. 34, no. 4, pp. 1443 – 1449, 2007.

[16] R. Taha Al-Kasasbeh, M. Salman Shamaseen, and D.E. Skopin, "Automated detection and selection of artifacts in encephalography signals", *Biomedical Engineering*, vol. 42, no. 6, pp. 293–301, 2008.

[17] A. Mognon, J. Jovicich, L. Bruzzone, and M. Buiatti, "ADJUST: an automatic EEG artifact detector based on the joint use of spatial and temporal features", *Psychophysiology*, vol. 48, no. 2, pp. 229 – 240, 2011.

[18] P.J. Durka, H. Klekowicz, K.J. Blinowska, W. Szelenberger, and S.Z. Niemcewicz, "A simple system for detection of EEG artifacts in polysomnographic recordings", *IEEE Transactions on Biomedical Engineering*, vol. 50, no. 4, pp. 526–528, 2003.

[19] S. Bhattacharyya, A. Biswas, J. Mukherjee, A.K. Majumdar, B. Majumdar, S. Mukherjee, and A.K. Singh, "Detection of artifacts from high energy bursts in neonatal EEG", *Computers in Biology and Medicine*, vol. 43, no. 11, pp. 1804 – 1814, 2013.

[20] S. Sanei and J.A. Chambers, *EEG Signal Processing*, Wiley, 2008.

[21] B. Boashash and N.A. Khan, "NPRP 4-1303-2-517, 6th monthly report", Tech. Rep., Qatar University, Cillege of Engineering, Doha, Qatar, June 2014.

[22] B.D. Forrester, *Time-Frequency Analysis in Machine Fault Detection*, chapter 18 in *Time–Frequency Signal Analysis: Methods and Applications*, B. Boashash, ed., pp. 406–423, Longman-Cheshire/Wiley, 1992.

[23] J. Löfhede, M. Thordstein, N. Löfgren, A. Flisberg, M. Rosa-Zurera, I. Kjellmer, and K. Lindecrantz, "Auto-

matic classification of background EEG activity in healthy and sick neonates.", *Journal of neural engineering*, vol. 7, no. 1, pp. 16007, Feb. 2010.

[24] B. Boashash and L. Boubchir, "On the selection of time–frequency features for improving the detection and classification of newborn EEG seizure signals and other abnormalities", in *19th International Conference on Neural Information Processing (ICONIP2012), Part IV, Lecture Notes in Computer Science (LNCS) 7666*, Nov. 2012, pp. 634–643.

[25] V. Sucic, N. Saulig, and B. Boashash, "Estimating the number of components of a multicomponent nonstationary signal using the short-term time-frequency Renyi entropy", *EURASIP Journal on Advances in Signal Processing*, vol. 2011, no. 1, pp. 1–11, 2011.

[26] B. Boashash, "Estimating and interpreting the instantaneous frequency of a signal. I. fundamentals", *Proceedings of the IEEE*, vol. 80, no. 4, pp. 520 –538, Apr. 1992.

[27] B. Boashash, "Estimating and interpreting the instantaneous frequency of a signal. II. algorithms and applications", *Proceedings of the IEEE*, vol. 80, no. 4, pp. 540 –568, Apr. 1992.

[28] H. Hassanpour, M. Mesbah, and B. Boashash, "Time–frequency feature extraction of newborn EEG seizure using SVD-based techniques", *EURASIP Journal on Applied Signal Processing*, vol. 2004, pp. 2544–2554, Jan. 2004.

[29] H. Kim and H. Park, "Nonnegative matrix factorization based on alternating nonnegativity constrained least squares and active set method", *SIAM Journal on Matrix Analysis and Applications*, vol. 30, no. 2, pp. 713–730, 2008.

[30] A. Temko, E. Thomas, W. Marnane, G. Lightbody, and G. Boylan, "EEG-based neonatal seizure detection with support vector machines", *Clinical Neurophysiology*, vol. 122, no. 3, pp. 464 – 473, 2011.

[31] B. Ghoraani and S. Krishnan, "Time–frequency matrix feature extraction and classification of environmental audio signals", *IEEE Transactions on Audio, Speech, and Language Processing* , vol. 19, no. 7, pp. 2197–2209, 2011.

[32] M.W. Berry, M. Browne, A.N. Langville, V.P. Pauca, and R.J. Plemmons, "Algorithms and applications for approximate nonnegative matrix factorization", *Computational Statistics & Data Analysis*, vol. 52, no. 1, pp. 155 – 173, 2007.

[33] E. Sejdic, I. Djurovic, and J. Jiang, "Time–frequency feature representation using energy concentration: An

overview of recent advances", *Elsevier Digital Signal Processing*, vol. 19, no. 1, pp. 153 – 183, 2009.

[34] L. Stankovic, "A measure of some time–frequency distributions concentration", *Signal Processing*, vol. 81, no. 3, pp. 621 – 631, 2001.

[35] B. Boashash and M. Ghafoor, "Time frequency signal analysis and processing toolbox update 6.2: An enhanced research platform with new advanced high–resolution TFDs", in *2013 8th International Workshop on Systems, Signal Processing and their Applications (WoSSPA)*, 2013, pp. 442–451.

[36] A. Aarabi, F. Wallois, and R. Grebe, "Automated neonatal seizure detection: A multistage classification system through feature selection based on relevance and redundancy analysis", *Clinical Neurophysiology*, vol. 117, no. 2, pp. 328–340, 2006.

[37] R.A. Shellhaas and R.R. Clancy, "Characterization of neonatal seizures by conventional EEG and single-channel EEG", *Clinical Neurophysiology*, vol. 118, no. 10, pp. 2156–2161, 2007.

[38] V. Lawhern, W.D. Hairston, K. McDowell, M. Westerfield, K. Robbins "Detection and classification of subject-generated artifacts in EEG signals using autoregressive models", *Journal of Neuroscience Methods*, vol. 208, no. 2, pp. 181–189, 2012.

[39] Z. Tiganj, M. Mboup, C. Pouzat, and L. Belkoura "An algebraic method for eye blink artifacts detection in single channel EEG recordings", in *17th International Conference on Biomagnetism Advances in Biomagnetism (Biomag2010)*, 2010, pp. 175–178.

[40] X. Yong, M. Fatourechi, R.K. Ward, G.E. Birch, "Automatic artefact detection in a self-paced brain-computer interface system", in *IEEE Pacific Rim Conference on Communications, Computers and Signal Processing (PacRim)*, 2011, pp. 403–408.

[41] F. Lotte, M. Congedo, A. Lécuyer, F. Lamarche, and B. Arnaldi, "A review of classification algorithms for EEG-based brain-computer interfaces", *Journal of neural engineering*, vol. 4, no. 2, Jun. 2007.

[42] B. Boashash, L. Boubchir, and G. Azemi, "A methodology for time–frequency image processing applied to the classification of non-stationary multichannel signals using instantaneous frequency descriptors with application to newborn EEG signals", *EURASIP Journal on Advances in Signal Processing*, vol. 2012, pp. 1–21, 2012.

[43] J. Nathalie and M. Shah, *Evaluating learning algorithms: A classification perspective*, Cambridge University Press, 2011

[44] B.R. Greene, S. Faul, W.P. Marnane, G. Lightbody, I. Korotchikova, and G.B. Boylan, "A comparison of

quantitative EEG features for neonatal seizure detection", *Clinical Neurophysiology*, vol. 119, no. 6, pp. 1248 – 1261, 2008.